Proceedings of the 26th International Conference on Offshore Mechanics and Arctic Engineering
OMAE2007
June 10-15, 2007, San Diego, California, USA

OMAE2007-29415

SIGNIFICANCE OF BIAXIAL STRESS ON THE STRAIN CONCENTRATION AND CRACK DRIVING FORCE IN PIPELINE GIRTH WELDS WITH SOFTENED HAZ

Ming Liu
Engineering Mechanics Corporation of Columbus
3518 Riverside Dr., Suite 202
Columbus, OH 43221, USA
mliu@emc-sq.com

Yong-Yi Wang
Engineering Mechanics Corporation of Columbus
3518 Riverside Dr., Suite 202
Columbus, OH 43221, USA
ywang@emc-sq.com

ABSTRACT

The effect of the biaxial stress and HAZ softening on the crack driving force of girth weld defects was investigated using finite element analyses (FEA). The defects were of elliptic shape and located on the inner surface of the pipe. The crack driving force is represented by the crack tip opening displacement (CTOD) normal to the cracked plane (Mode I). The effect of hoop stress on a homogeneous pipe was revisited at first. It was found that the application of hoop stress tends to increase the crack driving force. However, in the practical range of longitudinal strains ($\leq$4.0%), the effects of hoop stress is not monotonic. For example, at a constant longitudinal strain, as the pre-existing hoop stress increases, the driving force may firstly increase then decrease. The combined effect of HAZ softening and biaxial stress was then studied. With the application of hoop stress, the increase of the crack drive force due to HAZ softening was amplified. It was found that the crack driving force can be closely correlated with the surface strain measured over a structurally significant scale right above the defect. In addition, the effects of loading sequence and material anisotropy on the crack driving force were also briefly examined. The increase of the crack driving force from the hoop stress is more pronounced when it is applied prior to the application of longitudinal strains than the reverse loading sequence. The material anisotropy was found to further increase the crack driving force and therefore representative material models are necessary to analyze the anisotropy effects.

INTRODUCTION

Modern low-carbon micro-alloyed TMCP linepipe steels generally have high impact toughness and excellent weldability [1,2]. However, the lean chemistry of those steels also leads to some undesirable mechanical properties, such as low strain hardening capability and low uniform elongation. Due to the reduced hardenability, the welding thermal cycles may reduce the strength of the heat-affect-zone (HAZ) as compared to the base metal [2], which is termed HAZ softening. The HAZ softening is quite probable in modern micro-alloyed linepipes, particularly in the seam welds and the girth welds of double joints. Those undesired features can reduce the implicit safety margins in the available design codes, especially in strain-based design of pipelines. For instance, low strain hardening and low ductility are known to be detrimental to strain capacity [3,4,5,6,7,8].

The HAZ softening can cause/enhance strain concentration and potentially reduce the strain capacity of pipeline girth welds. The effect of HAZ softening on strain concentration and crack driving force was analyzed in [9]. Only longitudinal loading was considered in the previous work. However, in-service pipelines are subjected to hoop stress from the internal pressure, in addition to possible longitudinal loadings. A biaxial loading condition exists when the longitudinal loading is applied. The hoop stress can greatly alter the materials response to the longitudinal stress/strain. Therefore, the effect of the biaxial loading on girth weld integrity has drawn significant attentions in recent years [10,11,12,13,14,15].

The objective of this work was to understand the significance of biaxial loading on the integrity of pipeline girth welds with softened HAZ using a fundamental fracture mechanics approach. FEA models of a full size pipe containing surface-breaking defects located on the fusion boundary were analyzed. The effect of the biaxial stress was firstly investigated without any weld-metal mismatching or HAZ softening. The effect of the hoop stress on CTOD driving force is studied for different defect sizes and material properties. The softened HAZ is then introduced. The crack driving forces and local strains over a structurally significant finite-length scale were examined. Although thorough understanding on the significance of the biaxial stress and HAZ softening will require some well-executed experimental tests, the results provide some useful information to the strain-based design of pipelines under realistic service conditions.

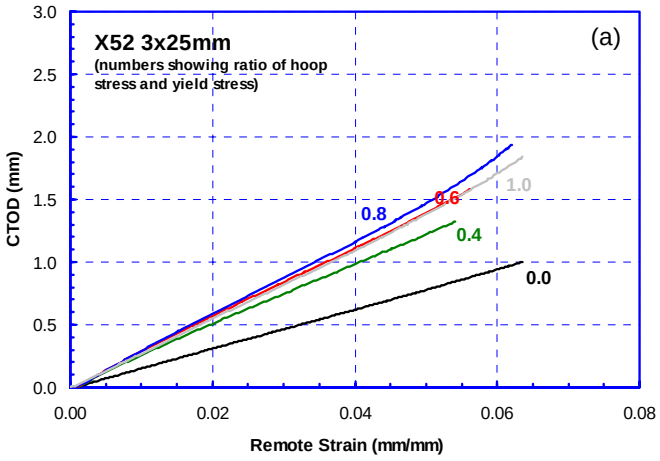

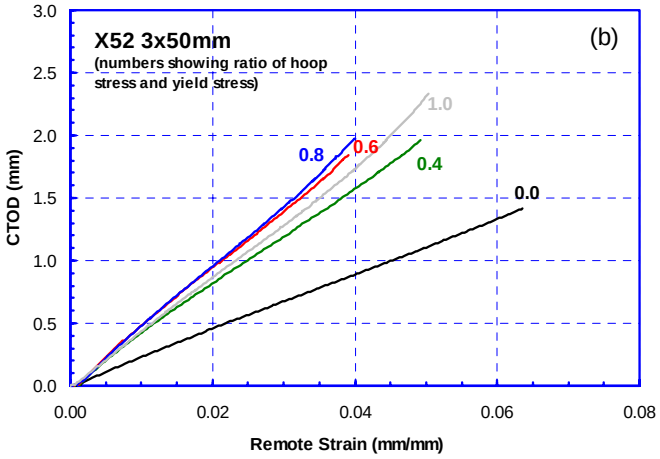

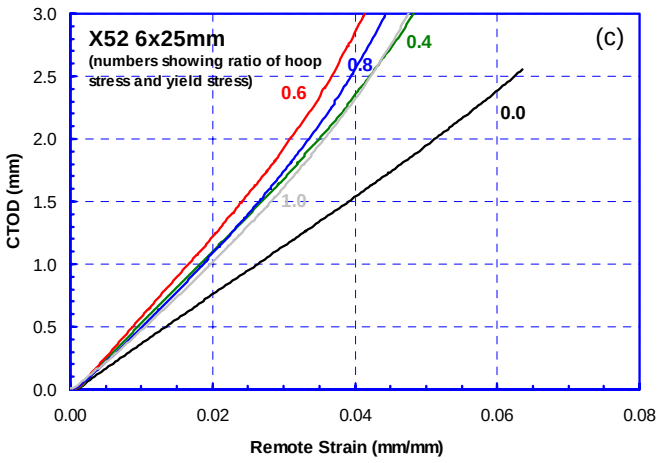

Figure 1 Effect of hoop stress on CTOD driving force curves of X52 pipe for defect size (depth (a) × length ($2c$)) (a) 3x25 mm (b) 3x50 mm (c) 6x25 mm.

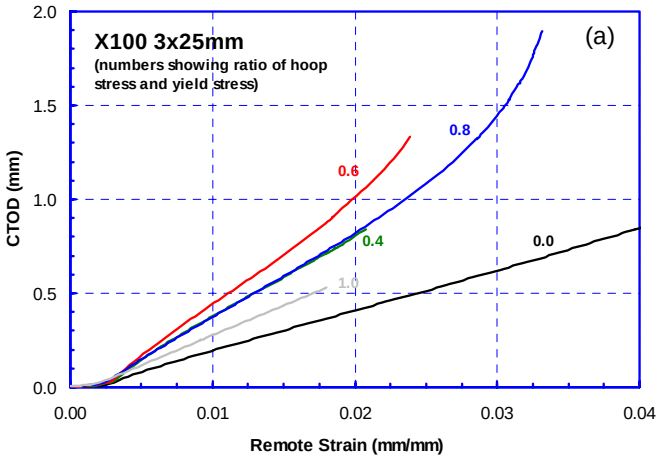

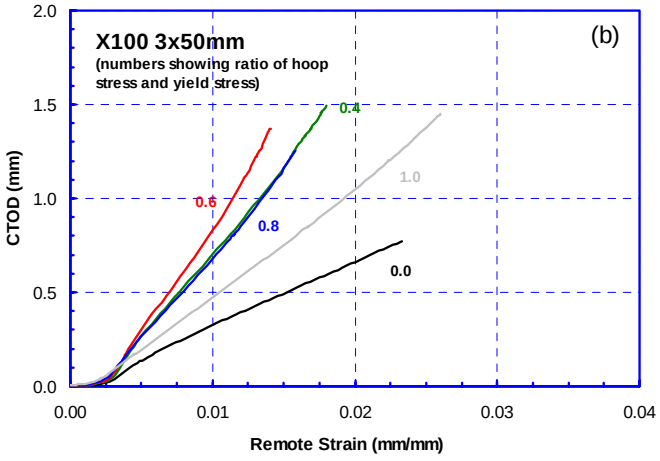

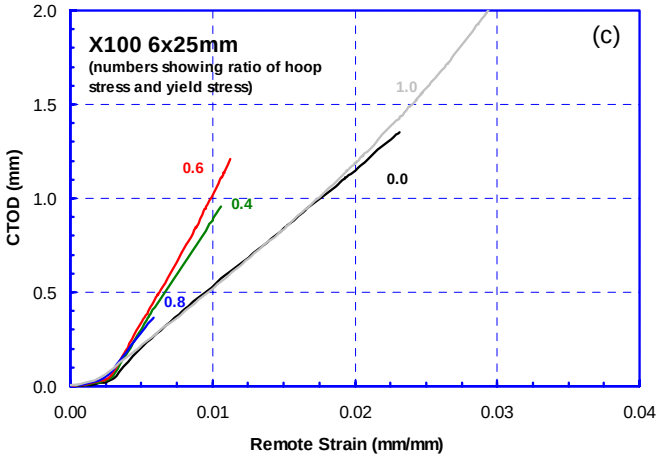

Figure 2 Effect of hoop stress on CTOD driving force curves of X100 pipe for defect size (a×$2c$) (a) 3x25 mm (b) 3x50 mm (c) 6x25 mm.

BIAXIAL STRESS EFFECT REVISIT

The effect of biaxial stress on the crack driving force of a surface breaking defect in a homogeneous pipe has been studied in recent years. It was generally observed that the hoop stress will increase the crack driving force. Therefore, in strain based design, the effect of the hoop stress needs to be properly considered.

In this section, the hoop stress effect on a homogeneous pipe was revisited by conducting three-dimensional (3D) FEA with ABAQUS®. The analyses were conducted with an increased hoop stress range and refined hoop stress intervals than the previous analyses. The response of the crack driving force to applied longitudinal strain is examined under gradually increasing hoop stress conditions.

Geometry and Finite Element Model

All pipes had 36" outside diameter (OD) and 12.7 mm wall thickness (WT). The total length of the model was 10·OD. Three defect sizes were analyzed, where the defect depth (a) × defect length ($2c$) were 3×25 mm, 3×50 mm, and 6×25 mm, respectively. The defects were semi-elliptic and located on the inner surface of the pipe.

The hoop stress was generated at first by applying internal pressure without the end cap effect. The tensile strain was then applied in the longitudinal direction while holding the pressure. The uniform longitudinal strain remote from the defect at the far end of the model was defined as the remote strain which was used to quantify the axial loading levels.

The CTOD driving force was calculated at the deepest point of the crack front by the 45°-line intersection method [3].

Material Properties

The stress-strain curve was assumed to obey the CSA Z662 relation [5,6,7],

$$\varepsilon = \frac{\sigma}{E} + \left(0.005 - \frac{X_g}{E}\right)\left(\frac{\sigma}{X_g}\right)^n, \qquad (1)$$

where, the ε and σ are strain and stress, respectively. The E is elastic modulus (set to 207 GPa), X_g is pipe grade or yield stress at 0.5% strain, and n is strain hardening exponent. The Poisson's ratio ν is set to 0.3. The uniform strain, ε_T was defined as a function of the strain hardening exponent n [3],

$$\varepsilon_T = \frac{2}{n}. \qquad (2)$$

Two pipe grades, X52 and X100, were analyzed. The strain hardening exponent n, as defined in Eq. (1), was assumed to be 19.88 and 45.75 for X52 and X100, respectively.

Results

The relationship between the CTOD driving force and the longitudinally applied remote strain for X52 pipe with different pre-existing hoop stresses is given in Figure 1 for three different defect sizes: (a) 3×25 mm, (b) 3×50 mm, and (c) 6×25 mm. Similar results for the X100 pipe are given in Figure 2. The CTOD curves are given for hoop stresses from $0.0\sigma_y$ to $1.0\sigma_y$, where σ_y is the yield stress which is the same as the specified minimum yield stress (SMYS). It is found that in general, the hoop stress increases the CTOD driving force. However, instead of a monotonic increase, as the hoop stress increases, the overall CTOD driving force curves are firstly increased then decreased. The level of the hoop stress that yields the highest CTOD driving force curve depends on the material properties and defect geometries. Generally speaking, the higher the strain-hardening capacity and the smaller the defect, the higher the hoop stress that yields the maximum crack driving force curve. Similar trend exists when the crack driving force is represented by the J-integral [16].

An example of the CTOD driving force curve at very low longitudinal strain range is shown in Figure 3 for the X100 pipe with 6×25 mm defect. It shows that at the initial (low) loading stage, higher hoop stress always results in higher CTOD driving force. The CTOD curves of different hoop stresses start to cross over as longitudinal strain increases. The observed phenomenon could be due to the competing effects of the hoop stress on the Von Mises stress and hydrostatic pressure (or stress tri-axiality). Higher pre-existing hoop stress always leads to higher initial Mises stress when there is no longitudinal strain. However, as the longitudinal strain increases, the stress tri-axiality increases and the Mises stress decreases. But once the longitudinal strain is beyond a threshold, the increase in longitudinal strain will increase the Mises stress. Therefore, although a lower hoop stress case starts from lower Mises stress, the threshold longitudinal strain for Mises stress to increase is lower than that of a higher hoop stress case. Therefore, at certain longitudinal strain, the lower hoop stress case starts to have a higher Mises stress and therefore higher crack driving forces. The stress tri-axiality depends on defect sizes and material properties, therefore the shift of the CTOD curves should also depend on the defects and materials.

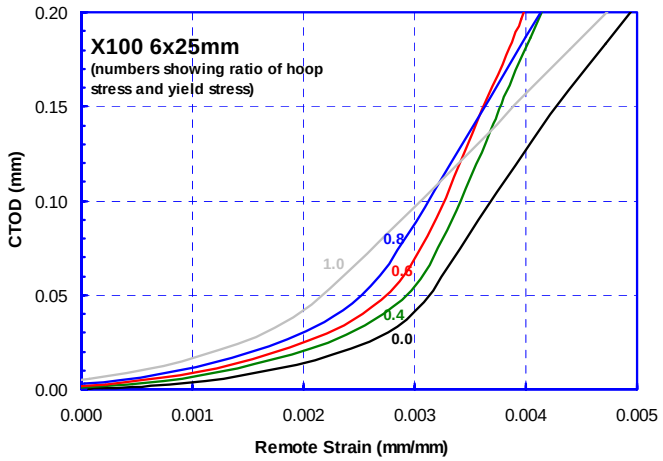

Figure 3 Effect of hoop stress on CTOD driving forces of X100 pipe with 6x25 mm defect: at small load.

BIAXIAL LOADING WITH SOFTENED HAZ

HAZ Softening Profile

The HAZ softening profiles were taken from a trial heat of early generation X100 pipeline steel (early 1990's generation). The Vickers micro-hardness across the girth weld of the X100 linepipe steel is given in Figure 4 [17]. The hardness was measured at the mid-thickness of the welds using a 500 g load. The HAZ softening is evident as shown in Figure 4, where the width of the HAZ is about 2 mm. The average hardness in base metal (BM) is about 260, while the lowest hardness in HAZ is 220, which corresponds to a 15% reduction (softening). The X100 steel has 0.06% carbon, IIW carbon equivalent (CE) of 0.439, and Pcm of 0.186; and is highly weldable per the Graville diagram [18]. It should be noted that the more recent vantage X100 girth welds made with appropriate welding procedures could have less HAZ softening for the same welding condition.

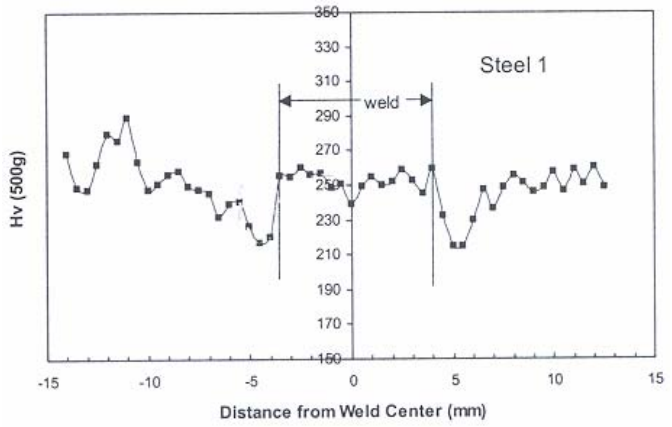

Figure 4 Micro-hardness traverse at mid-thickness of a micro-alloyed early generation trial heat of X100 pipeline steel [17]

Geometry and Finite Element Model

The overall pipe geometries were kept the same. The weld metal (WM) and HAZ modeled were 8 mm and 2 mm wide, respectively. The defects were located at the HAZ and WM boundary to simulate a lack-of-fusion flaw. Three defect sizes 3×25 mm, 3×50 mm, and 6×25 mm, were analyzed.

The FEA model is shown in Figure 5. Due to symmetry conditions, only half of the pipe was modeled. Details of the FEA mesh near the defect are shown in Figure 5, where the white, grey, and dark grey areas represent the BM, HAZ, and WM, respectively. The mesh on the WM side near the defect was removed in one figure to expose defect front. A key hole with a radius of 0.02 – 0.03 mm was created along the defect front for better convergence. A larger key-hole (0.04 mm radius) was also used in some cases for numerical convergence. The difference between the calculated CTOD using a 0.02 mm and 0.04 mm key hole is negligible.

Material Properties

The Young's modulus and Poisson's ratio were kept the same for BM, WM, and HAZ. The tensile properties of the BM and WM were also taken from a realistic girth weld of an experimental heat of X100 linepipe [19]. The BM stress-strain curve was measured using longitudinal direction full thickness specimens. The weld metal stress-strain curve was obtained from round-bar all-WM tensile tests. The stress-strain curves were given in Figure 6 and show a slightly WM overmatching (about 3%).

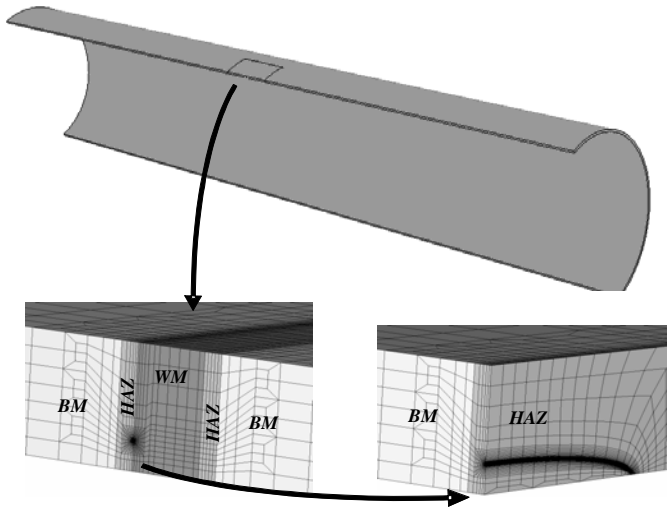

Figure 5 Finite element model of a pipe with a surface defect on the girth weld fusion boundary

The stress-strain curves of the HAZ materials were estimated by the following approach. The hardness profile in Figure 4 shows that the maximum degree of HAZ softening is about 15% compared to BM and the softest location is at the center of the HAZ. To simulate the material at the center of the HAZ, the yield and tensile strength of the BM were decreased by 15% and the whole stress-strain curve was also adjusted accordingly. The stress-strain curve representing 15% softened HAZ is also shown in Figure 6.

To represent the non-uniform distribution of material properties in HAZ, the materials in HAZ were modeled as functionally graded materials. The stress-strain curves of the material points within the HAZ were adjusted similarly as above according to their hardness levels. The material property distribution in HAZ is therefore similar to the hardness distribution. In addition, the BM, WM, and HAZ were all modeled as isotropic materials.

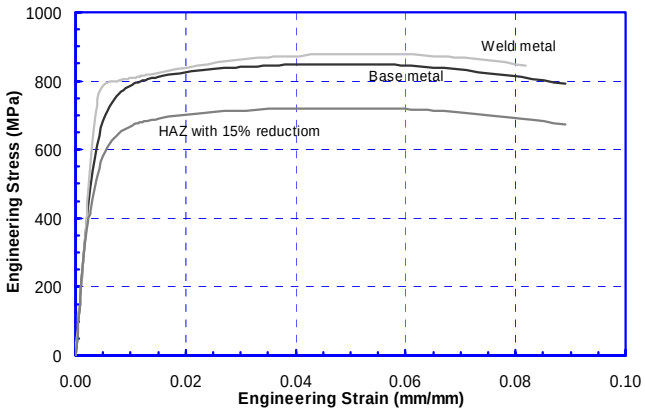

Figure 6 Stress-strain curves of BM, WM, and 15% softened HAZ

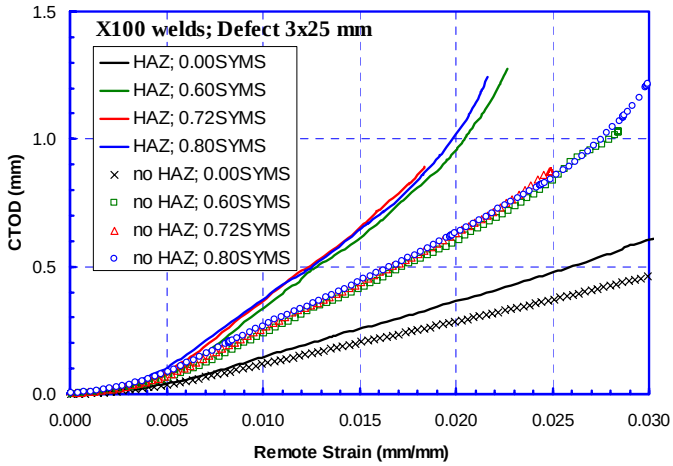

Figure 7 Effect of hoop stress on CTOD driving force with and without softened HAZ for defect 3×25 mm: all hoop stress levels

Definition of Strain Concentration

Strain concentration is sensitive to the location where it is measured, especially when defects exist. Therefore, a meaningful value of strain concentration can only be obtained over a realistic length scale. In our analyses, two strain measures were employed to demonstrate the strain concentration effect. First, the average strain over a 2*t* wide strip on the OD surface above the deepest point of the crack front was used and referred to as "2*t* surface strain". The 2*t* strip is used because it is just wide enough to contain the strain localization area on the OD surface induced by defects. In addition, the HAZ strain was defined as the average strain over the whole width of the HAZ remote from the defect (180^0 circumferentially from the center of the defect). If HAZ does not exist, the HAZ strain is actually the average strain over 2-mm wide BM strip adjacent to WM. The strain concentrations were calculated as the ratios between the above defined strains and the remote strain. The 2*t* surface strain is a measure of strain localization due to the defect, while the HAZ strain is a measure of strain localization in the HAZ due to the HAZ softening.

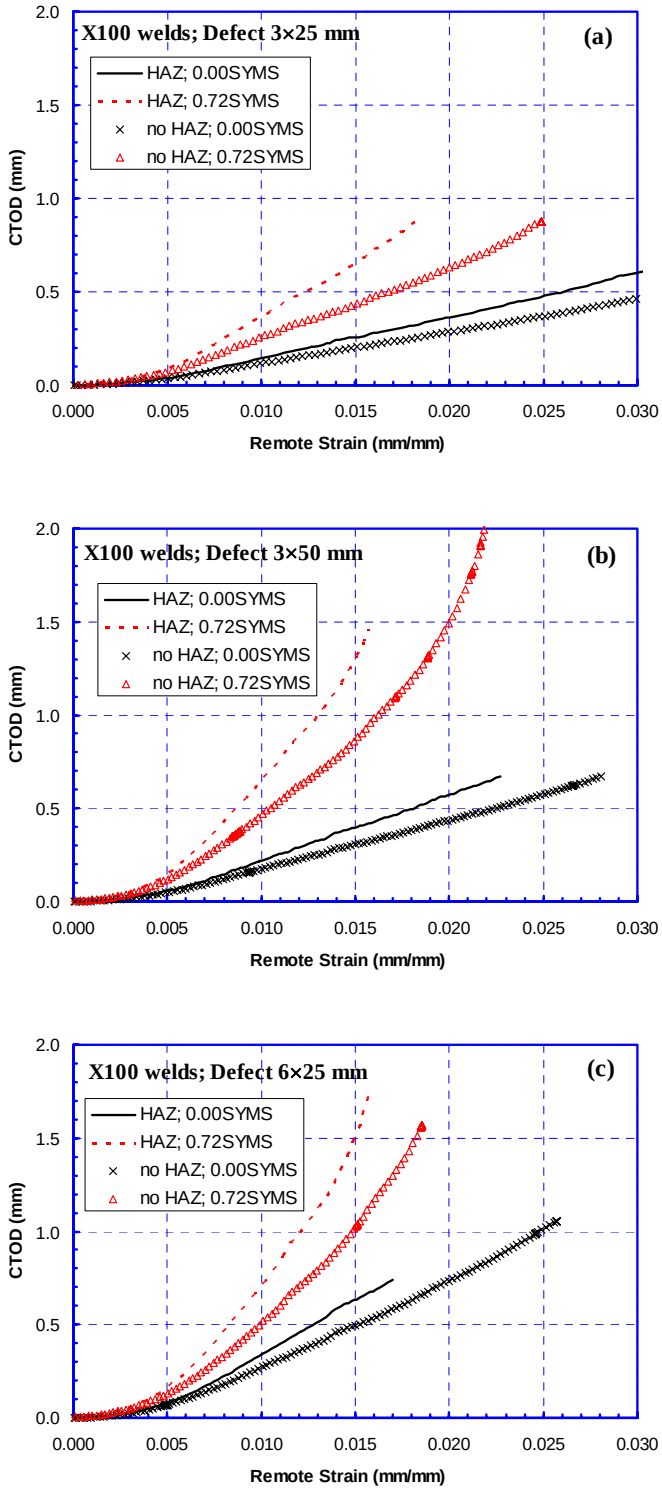

Figure 8 Effect of hoop stress on CTOD driving force with and without softened HAZ for defect (a) 3×25 mm (b) 3×50 mm; (c) 6×25 mm

CTOD Driving Forces

The total CTOD was the sum of the CTOD on the HAZ and WM side [9]. Three hoop stress levels, $0.60\sigma_y$, $0.72\sigma_y$, and $0.80\sigma_y$, were studied in our analyses. The hoop stress was generated at first by applying internal pressure where the end cap was not modeled. The tensile strain was then applied in the longitudinal direction with pressure holding constant. A typical result showing the relationship between the CTOD driving force and longitudinal strain is given in Figure 7 for defect size 3×25 mm. The result shows that for the materials used in our analyses, the hoop stress between $0.60\sigma_y$ and $0.80\sigma_y$, produces very similar crack driving forces. When longitudinal strain above 1.0% is considered, the hoop stress of $0.72\sigma_y$ yields the largest driving force. Similar observations are found on all three defect sizes. Therefore, in the following, only results at the hoop stress level of $0.72\sigma_y$ will be presented.

The CTOD driving force curves with and without hoop stress and softened HAZ are given in Figure 8. As expected, it shows that both softened HAZ and pre-exist hoop stress increase the CTOD driving force. For materials used in our analyses, the relative increase of CTOD driving force due to softened HAZ is not sensitive to defect sizes. As shown in Figure 9, at 1.5% remote strain, a 2-mm wide 15% softened HAZ increases the CTOD driving force by 30% if no hoop stress is applied. The pre-exist hoop stress magnifies the HAZ softening effect. At the same conditions but with a hoop stress of $0.72\sigma_y$, the softened HAZ increases the CTOD driving force by 50%.

Compared to the influence of HAZ softening, the hoop stress has a much greater effect on the CTOD driving force and its effect is very sensitive to defect size. Although the total CTOD driving force is more affected by defect depth than length, the hoop stress seems to have larger effect on longer defects than deeper defects. For example, of all three defect sizes studied in this paper, the deepest defect (6×25 mm) always has the largest CTOD driving force for the same conditions. However, at 1.5% strain and no softened HAZ, the hoop stress of $0.72\sigma_y$ increases the CTOD driving force by 180% for the longest defect (3×50 mm) , and only 110% for the shorter defects (3×25 mm and 6×25 mm). When a 2-mm wide 15% softened HAZ exists, the CTOD driving force will be increased by the hoop stress by 230% for the 3×50 mm defect and 150% for the 3×25 mm and 6×25 mm defects, respectively.

Due to the strength mismatching, the crack tip opening in HAZ and WM is not symmetric. The opening mode, ratio between the CTOD in HAZ side ($CTOD_{HAZ}$) and the total CTOD, is shown in Figure 10. Those plots show the extent of preferential deformation in the softened HAZ near the defect. For the cases without HAZ, the curve shows the fraction of the CTOD on the BM side, where due to slightly WM overmatching, the CTOD on the BM side is higher than that on the WM side. The initial variations of the curves are mainly caused by the yielding sequences of the HAZ, BM, and WM [9]. Figure 10 shows that, without hoop stress and softened HAZ, the asymmetry caused by the 3% WM overmatching is relatively small. However, the softened HAZ increase the asymmetry significantly and the hoop stress can further increase the asymmetry. The extent of asymmetry does not seem to be very sensitive to defect sizes, although the results show that a longer defect can have a larger asymmetric opening.

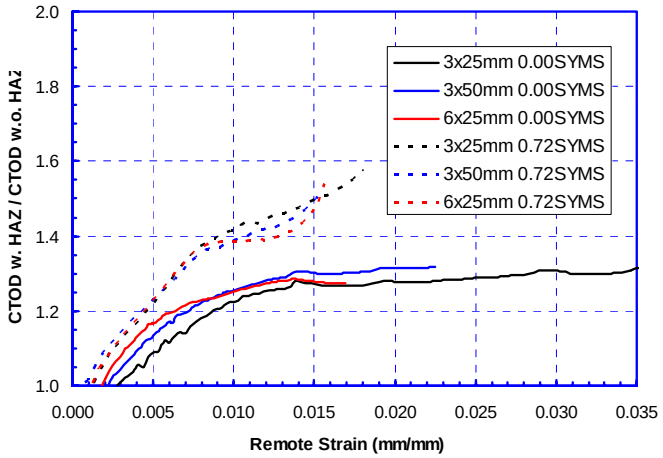

Figure 9 Amplification of CTOD due to softened HAZ with and without hoop stress for various defect sizes

Strain Concentration

The effect of hoop stress and HAZ softening on the 2*t* surface strain concentration is given in Figure 11. It shows that the HAZ softening and hoop stress have similar effects on the 2*t* surface strain with that on the CTOD driving force. The relationship between the CTOD driving force and 2*t* surface strain for various defects is given in Figure 12. It can be seen that a linear relation exists for all the cases. Furthermore, the slope of the linear relationship is not sensitive to defect sizes and HAZ softening when high hoop stress exists. While a weak dependence on defect sizes and HAZ softening can be found when no hoop stress exists. It clearly indicates that the 2*t* surface strain can be used as a convenient method for measuring the CTOD driving force in practical experiment, especially for a full-size pipe with internal pressure applied.

On the other hand, Figure 13 shows that the HAZ strain concentration, although might be intuitively taken to be a reasonable measure of the CTOD driving force, does not correlate with the CTOD driving force. For example, at 1.5% remote strain, a strain concentration in the HAZ (2-mm wide and 15% softened) of 2% and 23% was found for the cases without and with hoop stress, respectively. It does not correlate with the 30% and 50% corresponding increase in CTOD driving force. It is especially true when HAZ does not exist. The results show the applied hoop stress decreases the strain concentration, while the CTOD driving force is greatly increased by the hoop stress. The strain level in the HAZ near the defect is very different from that remote from the defect. Since the materials behave very differently at those different strain levels, the deformation in HAZ without defect and therefore the HAZ strain concentration, can not represent the deformation near a defect.

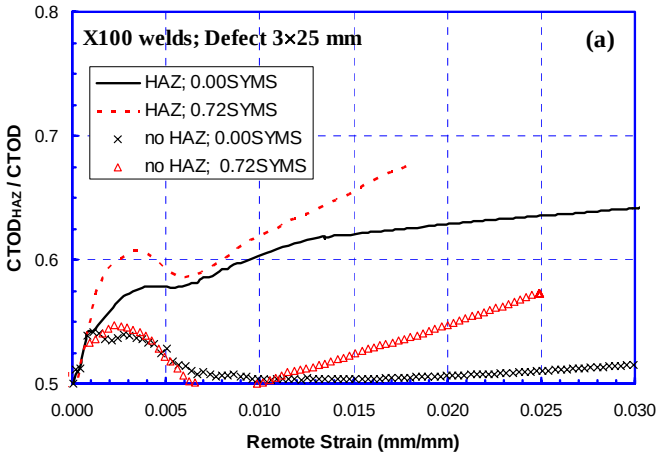

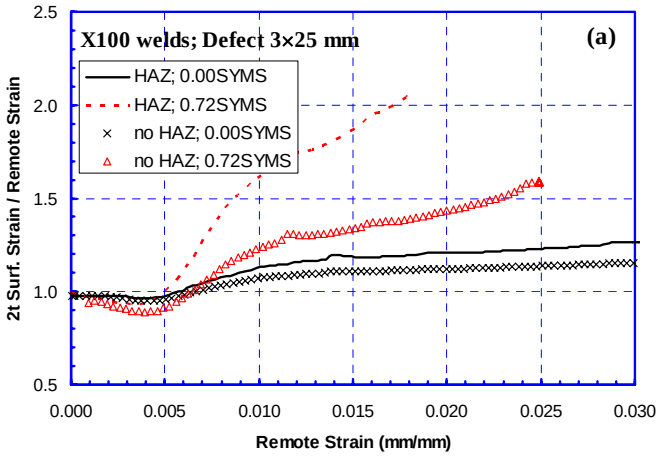

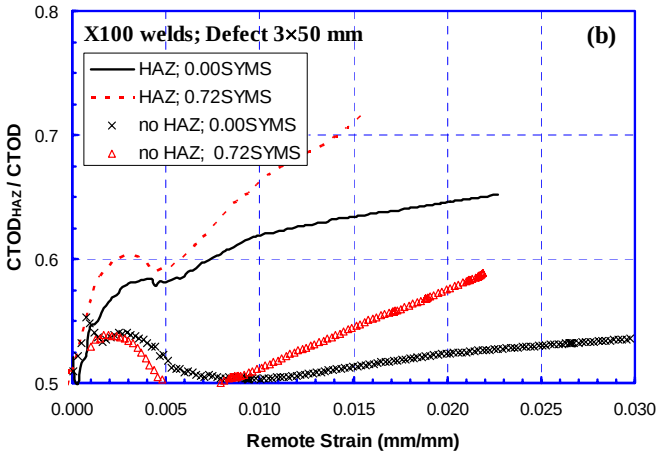

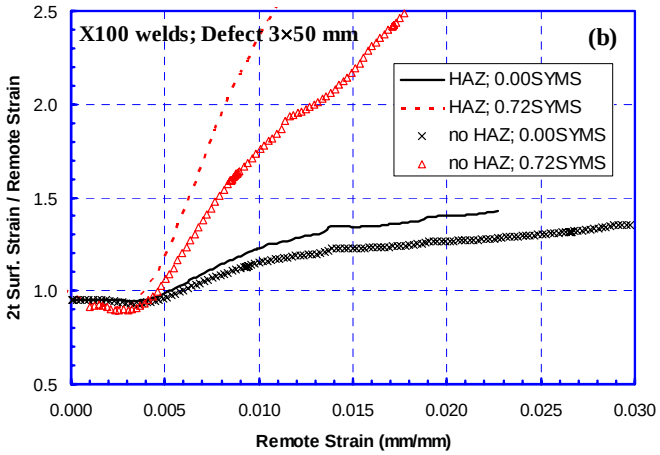

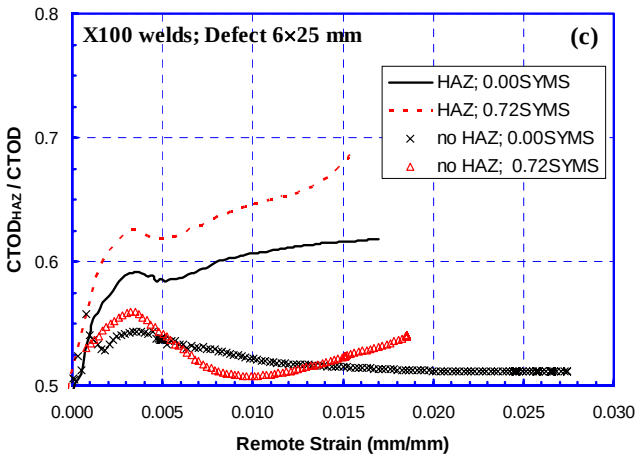

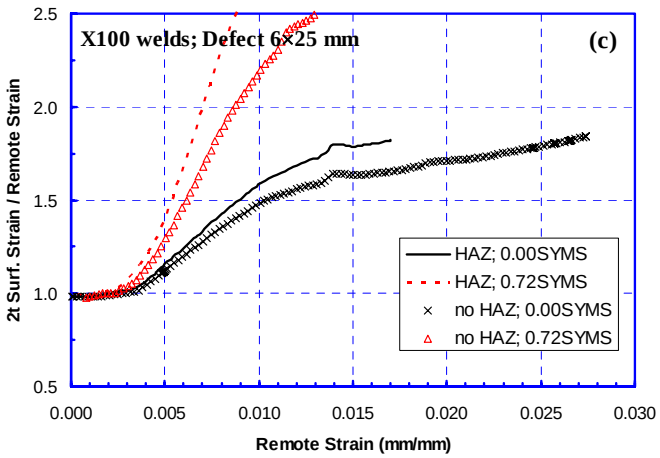

Figure 10 Effect of hoop stress on CTOD opening mode with and without softened HAZ for defect (a) 3×25 mm (b) 3×50 mm; (c) 6×25 mm

Figure 11 Effect of hoop stress on 2*t* strain concentration with and without HAZ for defect (a) 3×25 mm (b) 3×50 mm; (c) 6×25 mm

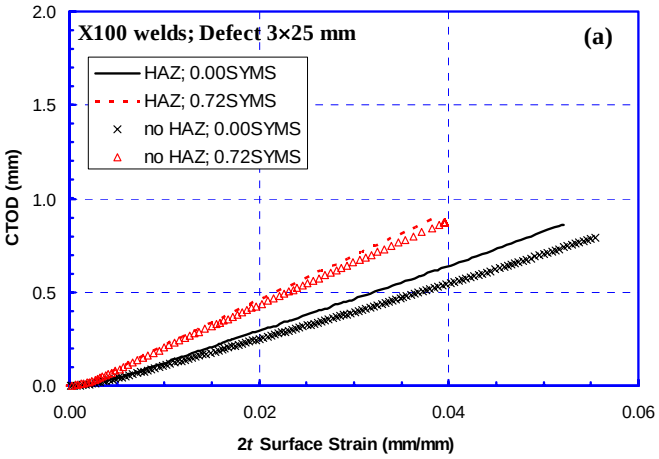

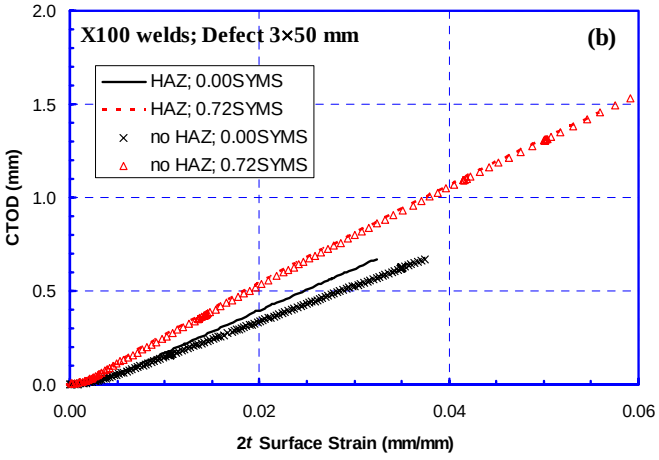

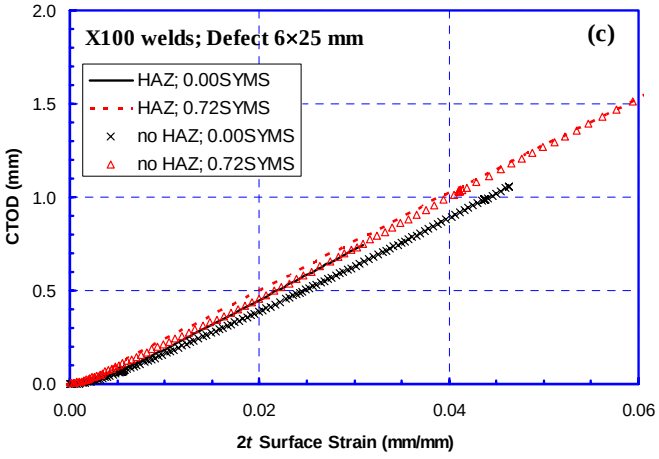

Figure 12 Relationship between CTOD driving force and 2*t* surface strain with and without softened HAZ for defect (a) 3×25 mm (b) 3×50 mm; (c) 6×25 mm

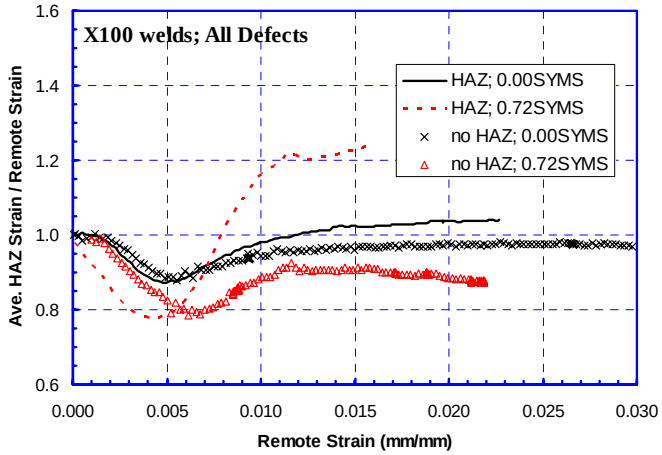

Figure 13 Effect of hoop stress on average HAZ strain concentration with and without softened HAZ

DISCUSSION

Effects of Loading Sequence

It is well known that the plastic deformation depends on loading history/sequence. In field service, the pipeline usually experiences longitudinal strains after the hoop stress has been applied. However, other loading sequence might happen. Figure 14 shows the effect of loading sequence on the CTOD driving force. In Figure 14, two cases, (1) hoop stress applied before longitudinal strain and (2) hoop stress applied after longitudinal strain, were analyzed. The results show that the CTOD driving force generated by the hoop stress applied after longitudinal strain is much smaller than that generated by the pre-existing hoop stress. For an example, at 1.0% strain, the CTOD driving force is increased from 0.21 mm to 0.36 mm by the hoop stress if the longitudinal strain is applied first. The CTOD is increased to 0.65 mm if the hoop stress is applied first.

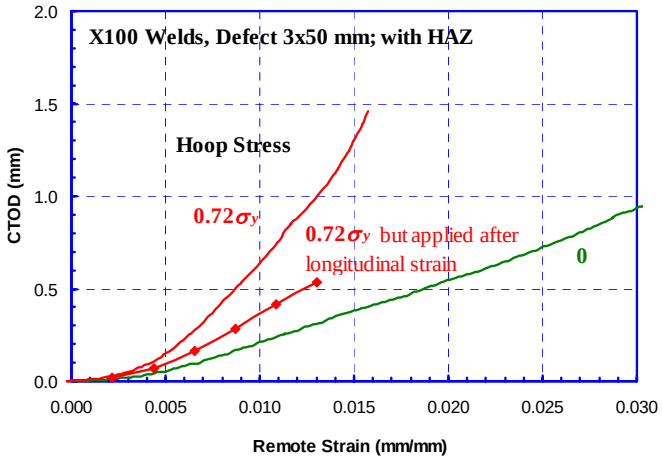

Figure 14 Effect of loading sequence on CTOD driving force for defect 3x50 mm

Effects of Anisotropic Material Properties

The longitudinal and transverse tensile properties of the modern TMCP and UOE linepipe steels can be quite different due to the texture created during rolling and cold work applied in pipe manufacturing. For example, the stress-strain curves of an X100 steel in transverse and longitudinal directions are shown in Figure 15. It is seen that the yield strength in the transverse direction is much higher than that in the longitudinal direction. However, the strain hardening capacity in the transverse direction is much lower than that in the longitudinal direction. It should be noted that the ultimate tensile strengths (UTS) of this steel in both directions are very close. Therefore this anisotropy can be modeled reasonably well with the isotropic/kinematic hardening model as seen in Figure 15. The details of the model and the tuning of the model were given in [20]. For some steels, the UTS of different directions can be different and more representative material models must be used.

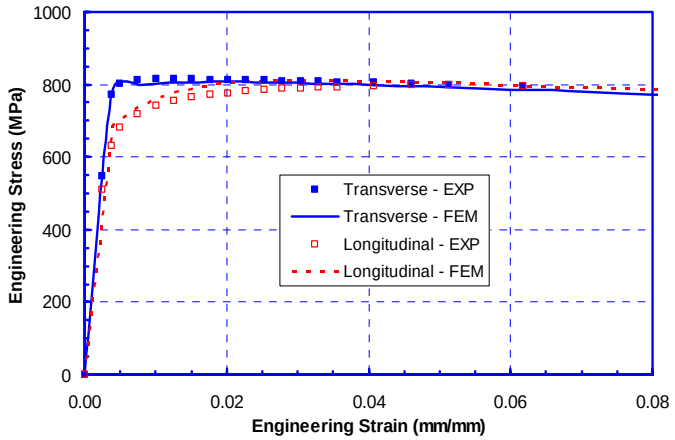

Figure 15 Anisotropic stress-strain behavior of an X100 pipe steel

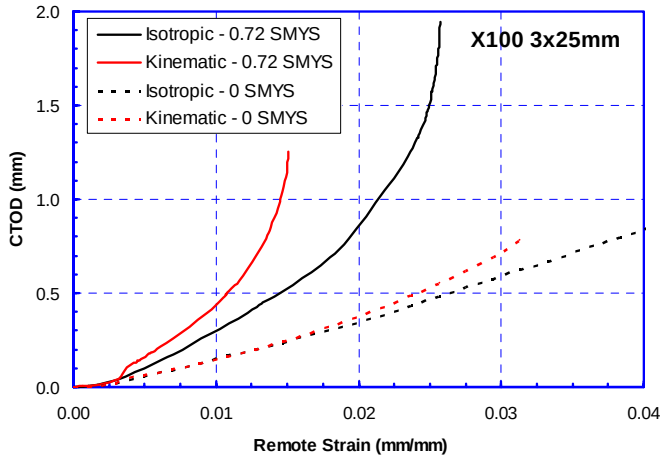

Figure 16 Effect of materials anisotropy on calculated CTOD driving force for defect 3x25 mm

To study the effect of the material anisotropy on the crack driving force, two material models were used. The first one was the conventional isotropic hardening model which is the same as that used in the rest of the paper, i.e., the stress-strain behaviors in all directions are assumed to be the same. In this model, the stress-strain curve in the longitudinal direction was used since this is the direction where the load was applied. The second model was the above mentioned isotropic/kinematic hardening model. The model was tuned to be able to simulate the stress-strain relations in both transverse and longitudinal directions reasonably well [20]. The calculated CTOD driving force curves are shown in Figure 16. Without hoop stress, the two material models produced very similar results at low applied strain but the difference increases as the applied strain increases. However, when hoop stress is applied, the CTOD driving force calculated from the isotropic/kinematic hardening model is much higher than that calculated from the isotropic model. The reduced material hardenability in the transverse direction could be responsible for the elevated driving force.

CONCLUSIONS

In the beginning of the paper, the effect of hoop stress on the crack driving force of a girth weld defect in a homogeneous pipe under longitudinal strain load was briefly studied. As observed in other similar work, it was found that the application of the hoop stress generally increases the crack driving force by a significant amount. However, in this paper for the first time, it was found that the effect of the hoop stress is not monotonic. When the longitudinal strain is low, a higher hoop stress always yields higher driving force. However, if the strain of the longitudinal direction is beyond certain values, as the hoop stress increases from 0.0 to $1.0\sigma_y$, the crack driving force increases at first, and then decreases. Therefore, a threshold hoop stress exists, at which the crack driving force at certain longitudinal strain is maximized. This threshold value is dependent of defect sizes and material stress-strain properties.

Detailed FEA were then conducted to investigate the effect of biaxial stress on crack driving force and strain concentration in pipeline girth welds with softened HAZ. The material properties of WM and BM were obtained from an actual X100 girth weld. The softened HAZ was modeled as a functionally graded material based on measured hardness profile.

For the combination of the material properties studied and for a range of defect sizes, it was found that a hoop stress of $0.72\sigma_y$ always yields CTOD driving force close to the maximum when the longitudinal strains is above 1%. It was also found that the application of the hoop stress magnifies the effect of the HAZ softening. For example, at 1.5% remote strain, a 2-mm wide and 15% softened HAZ alone can increase the CTOD driving force by 30% compared to a homogenous pipe. With a hoop stress of $0.72\sigma_y$ being applied, the same HAZ can increase the CTOD driving force by 50%. On the other hand, the existence of softened HAZ also magnifies the effect of hoop stress on the crack driving force. Although the magnitude of the crack driving force is more affected by defect depth, the relatively increase of the CTOD driving force by hoop stress is more sensitive to defect length. For instance, at 1.5% remote strain when a softened HAZ exists, although the CTOD driving force of a 6×25 mm defect is larger than that of a 3×50 defect, the application of a $0.72\sigma_y$ hoop stress increases the driving force by 150% for the 6×25 mm defect. In comparison a 230% increase is observed for the 3×50 mm defect.

The strain concentration in the HAZ due to softening was found not to correlate well with the CTOD driving force. A $2t$

surface strain concentration defined by the authors seems to be a convenient parameter for measuring the relative effects of hoop stress and HAZ softening on CTOD driving force.

The potential effect of loading sequence and material anisotropy were also discussed. The results showed that the pre-exist hoop stress applied before longitudinal strain has a much larger effect on the CTOD driving force than the hoop stress applied after the longitudinal strain does. Furthermore, it was found that the cold work applied by pipe manufacturing process such as UOE can increase the yield strength but reduce the strain hardening capacity in the transverse direction. The CTOD driving force can be increased by a large amount due to the resulting material anisotropy, especially when hoop stress is applied. To properly consider this effect, a better material model other than the isotropic hardening model must be used. The effect of anisotropy warranties more investigation.

ACKNOWLEDGMENTS

The work is supported by U.S. Department of Energy (DOE) under Agreement DE-FC36-04GO14040 and the Pipeline Research Council International (PRCI). The support of TransCanada Pipelines, Ltd. in providing test data and other materials is greatly appreciated.

REFERENCES

1 Hillenbrand, H., et al., "Development of large-diameter pipe in grade X100 – State-of-the-art report from the manufacture's point of view," *Pipeline Technology*, ed. R. Denys, vol. 1, pp. 469-482, 2000.

2 Ohm, R.K., Martin, J.T., and Orzessek, K.M., "Characterization of ultra high strength linepipe", *Pipeline Technology*, ed. R. Denys, vol. 1, pp. 483-496, 2000.

3 Wang, Y.-Y., et. al., "Tensile Strain Limits of Girth Welds with Surface-Breaking Defects Part I an Analytical Framework," *Proc. of the 4th International Conference on Pipeline Technology*, pp.235-249, Ostend, Belgium, May 9-13, 2004.

4 Wang, Y.-Y., et al., "Tensile Strain Limits of Girth Welds with Surface-Breaking Defects Part II Experimental Correlation and Validation" *Proc. of the 4th International Conference on Pipeline Technology*, pp.251-266, Ostend, Belgium, May 9-13, 2004.

5 Wang, Y.-Y., Cheng, W., and Horsley, D., "Tensile Strain Limits of Buried Defects in Pipeline Girth Welds," *Proc. of the 5th International Pipeline Conference*, Calgary, Alberta, Canada, October 4-8, 2004.

6 Denys, R., De Waele, W., Lefevre, A., and De Baets, P., "An Engineering Approach to the Prediction of the Tolerable Defect Size for Strain-Based Design," *Proc. of the 4th International Conference on Pipeline Technology*, pp. 163-181, Ostend, Belgium, May 9-13, 2004.

7 Denys, R., De Waele, W., Lefevre, A., and De Baets, P., "Plastic Straining Capacity of Axially-Loaded Pipelines: Experimental Facts and Critical Considerations," *Proc. of the 4th International Conference on Pipeline Technology*, pp. 183-207, Ostend, Belgium, May 9-13, 2004.

8 Denys, R., Lefevre, A., De Baets, P., and Degrieck, J., "Effects of Stable Ductile Crack Growth on Plastic Collapse Defects Assessments," *Proc. of the 3rd International Conference on Pipeline Technology*, Brugge, Belgium, May 21-24, 2000.

9 Liu, M., Wang, Y.-Y., and Horsley, D., "Significance of HAZ softening on strain concentration and crack driving force in pipeline girth welds", *Proc. of 24th International Conference on Offshore Mechanics and Arctic Engineering*, OMAE2005-67039, Halkidiki, Greece, June 12-16, 2005.

10 Wang, Y.-Y., Liu, M., and Horsley, D. J., "Some Aspects of Material and Welding Specifications for Strain-Based Design of Pipelines", *Proc. of EPRG-PRCI-APIA 15th Joint Technical Meeting on Pipeline Research*, Orlando, FL, USA, May 17-19, 2005.

11 Jayadevan, K.R., Ostby, E., and Thaulow, C., "Fracture response of pipelines subjects to large plastic deformation under tension" *Int. J. Pressure Vessels and Piping*, vol.81, pp 771-783, 2004.

12 Ostby, E., Jayadevan, K.R., and Thaulow, C., "Fracture response of pipelines subjects to large plastic deformation under bending" *Int. J. Pressure Vessels and Piping*, vol.82, pp 201-215, 2005.

13 Brumovsky, M., Lauerova, D., and Palyza, J., "Testing of fracture toughness under biaxial loading" *Proc. of the 2005 ASME Pressure Vessels and Piping Conference*, PVP2005-71479, Denver, CO, USA, July 17-21, 2005.

14 Shen, G., and Tyson, W.R., "Effect of biaxial stress on crack driving force" *Proc. of 2006 ASME Pressure Vessels and Piping Conference*, PVP2006-ICPV11-93849, Vancouver, BC, Canada, July 23-27, 2006.

15 Mohr, W., "Weld Area Mismatch and Pressure Effects in Strain-Based Design," *Proc. of the 4th International Conference on Pipeline Technology*, Ostend, Belgium, May 9-13, 2004, pp. 279-290.

16 Rice, J., "A path independent integral and the approximate analysis of strain concentration by notches and cracks", *J. Appl. Mech*., vol. 35, pp 379-386, 1968.

17 Wang, Y.-Y. and Rapp, S., "Weldability of High Strength and Enhanced Hardenability Steels," *Proc. of 5th International Pipeline Conference*, IPC04-0526, vol. 2, pp. 1521-1528, Calgary, Alberta, Canada, October 4-8, 2004.

18 Graville, B.A., "Cold cracking in welds in HSLA steels," *Welding of HSLA Microalloyed Structural Steels*, ASM, Rome, Italy, Nov, 1976.

19 Wang, Y.-Y., Liu, M., and Cheng, W.T., An internal report to TransCanada Pipelines Ltd., 2004.

20 Liu, M. and Wang, Y.-Y., "Modeling of anisotropy of TMCP and UOE linepipes", *Proc. of 16th International Offshore and Polar Engineering Conference*, San Francisco, CA, USA, May 28-June 2, 2006.